JNeurosci
THE JOURNAL OF NEUROSCIENCE

Research Articles: Behavioral/Cognitive

Neuroanatomy of the vmPFC and dlPFC predicts individual differences in cognitive regulation during dietary self-control across regulation strategies

Liane Schmidt[1], Anita Tusche[2], Nicolas Manoharan[3], Cendri Hutcherson[4,5], Todd Hare[6,7] and Hilke Plassmann[8,9]

[1]*Institute du Cerveau et de la Moelle Epinière, UMR 7225, U1127, INSERM/CNRS/UPMC, Hôpital Pitié-Salpêtrière, 75013 Paris, France*

[2]*Division of the Humanities and Social Sciences, California Institute of Technology, Pasadena, CA 91125, U.S.A.*

[3]*Sorbonne-Universités-INSEAD Behavioural Lab, INSEAD, 75005 Paris, France*

[4]*Department of Psychology, University of Toronto Scarborough, Canada*

[5]*Department of Marketing, Rotman School of Management, University of Toronto, Canada*

[6]*Laboratory for Social and Neural Systems Research, Department of Economics, University of Zurich, Zurich, Switzerland*

[7]*Neuroscience Center Zurich, University of Zurich, Swiss Federal Institute of Technology Zurich, Zurich, Switzerland*

[8]*Marketing Area, INSEAD, 77305 Fontainebleau, France*

[9]*INSERM, U960 Laboratoire de Neuroscience Cognitive, Ecole Normale Supérieure, 75005 Paris, France*

DOI: 10.1523/JNEUROSCI.3402-17.2018

Received: 1 December 2017

Revised: 12 April 2018

Accepted: 15 May 2018

Published: 4 June 2018

Author contributions: L.S., A.T., N.M., C.H., T.H., and H.P. performed research; L.S. and N.M. analyzed data; L.S. wrote the first draft of the paper; L.S. edited the paper; L.S., A.T., C.H., T.H., and H.P. wrote the paper; A.T., C.H., T.H., and H.P. designed research.

Conflict of Interest: The authors declare no competing financial interests.

The study was supported by the ANR Sorbonne Universités Emergence Grant awarded to HP. The authors declare no competing financial interest.

Correspondence should be addressed to Liane Schmidt, Institute du Cerveau et de la Moelle Epinière, Hôpital Pitié-Salpêtrière, 47 Blvd. de l'Hôpital, 75013 Paris, France. Email: liane.schmidt@icm-institute.org

Cite as: J. Neurosci ; 10.1523/JNEUROSCI.3402-17.2018

TITLE

Neuroanatomy of the vmPFC and dlPFC predicts individual differences in cognitive regulation during dietary self-control across regulation strategies

SHORT TITLE

Neuroanatomy predicts dietary self-control

Authors and affiliations

Liane Schmidt[*1], Anita Tusche[2], Nicolas Manoharan[3], Cendri Hutcherson[4,5], Todd Hare[6,7], and Hilke Plassmann[8,9]

[1]Institute du Cerveau et de la Moelle Epinière, UMR 7225, U1127, INSERM/CNRS/ UPMC, Hôpital Pitié-Salpêtrière, 75013 Paris, France
[3]Division of the Humanities and Social Sciences, California Institute of Technology, Pasadena, CA 91125, U.S.A.
[3]Sorbonne-Universités-INSEAD Behavioural Lab, INSEAD, 75005 Paris, France
[4]Department of Psychology, University of Toronto Scarborough, Canada
[5]Department of Marketing, Rotman School of Management, University of Toronto, Canada
[6]Laboratory for Social and Neural Systems Research, Department of Economics, University of Zurich, Zurich, Switzerland
[7]Neuroscience Center Zurich, University of Zurich, Swiss Federal Institute of Technology Zurich, Zurich, Switzerland
[8] Marketing Area, INSEAD, 77305 Fontainebleau, France
[9]INSERM, U960 Laboratoire de Neuroscience Cognitive, Ecole Normale Supérieure, 75005 Paris, France

[*]Correspondence should be addressed to Liane Schmidt, Institute du Cerveau et de la Moelle Epinière, Hôpital Pitié-Salpêtrière, 47 Blvd. de l'Hôpital, 75013 Paris, France. Email: liane.schmidt@icm-institute.org

Number of pages: 28
Number of figures: 3
Number of words: abstract (209); introduction (637); discussion (1141)

Acknowledgments

The study was supported by the ANR Sorbonne Universités Emergence Grant awarded to HP. The authors declare no competing financial interest.

Author contributions

H.P., A.T., C.H., and T.H. conceived the respective experiments and developed their experimental design. A.T., L.S., N.M., C.H., and T.H. collected the data; L.S. analyzed the data; N.M. assisted in data analysis; H.P., A.T., C.H., and T.H.

supervised the data analysis. L.S. and H.P. wrote the first draft of the manuscript, and all authors contributed to the final text.

Key words
valuation, ventromedial prefrontal cortex, dorsolateral prefrontal cortex, cognitive, regulation success, dietary self-control, voxel-based morphometry, neuroanatomy, gray matter volume, decision neuroscience, open science

Abstract

Making healthy food choices is challenging for many people. Individuals differ greatly in their ability to follow health goals in the face of temptation, but it is unclear what underlies such differences. Using voxel-based morphometry (VBM), we investigated in healthy humans (i.e., men and women) links between structural variation in gray matter volume and individuals' level of success in shifting toward healthier food choices. We combined MRI and choice data into a joint dataset by pooling across three independent studies that employed a task prompting participants to explicitly focus on the healthiness of food items before making their food choices. Within this dataset, we found that individual differences in gray matter volume in the ventromedial prefrontal cortex (vmPFC) and dorsolateral prefrontal cortex (dlPFC) predicted regulatory success. We extended and confirmed these initial findings by predicting regulatory success out of sample and across tasks in a second dataset requiring participants to apply a different regulation strategy that entailed distancing from cravings for unhealthy, appetitive foods. Our findings suggest that neuroanatomical markers in the vmPFC and dlPFC generalized to different forms of dietary regulation strategies across participant groups. They provide novel evidence that structural differences in neuroanatomy of two key regions for valuation and its control, the vmPFC and dlPFC, predict an individual's ability to exert control in dietary choices.

Significance statement

Dieting involves regulating food choices in order to eat healthier foods and fewer unhealthy foods. People differ dramatically in their ability to achieve or maintain this regulation, but it is unclear why. Here, we show that individuals with more gray matter volume in the dorsolateral and ventromedial prefrontal cortex are better at exercising dietary self-control. This relationship was observed across four different studies examining two different forms of dietary self-regulation, suggesting that neuroanatomical differences in the vmPFC and dlPFC may represent a general marker for self-control abilities. These results identify candidate neuroanatomical markers for dieting success and failure, and suggest potential targets for therapies aimed at preventing or treating obesity and related eating disorders.

Introduction

Humans have a remarkable capacity to utilize various cognitive regulation strategies to attain desired goals and to exercise self-control (Kober et al., 2010). Self-control dilemmas are often characterized by a trade-off between an immediate, tempting reward and a delayed, more abstract one (e.g., eat a piece of tasty chocolate cake now or forgo the pleasure to achieve better health and a longer life in the future; McClure et al., 2004; Kable and Glimcher, 2007; Hare et al., 2009, 2011; Li et al., 2013). Such decisions about diet, exercise, and other reward-guided behaviors all have consequential long-term effects on health and well-being. However, many people struggle to consistently stick to their diets, exercise, and save for retirement. A key challenge for promoting healthy, adaptive decision-making is understanding what underlies individual differences in self-control success (Tangney et al., 2004; Saarni et al., 2006; Pietilaeinen et al., 2011; Holmes et al., 2016).

Recent work in cognitive neuroscience has investigated this question by examining how individual differences in functional brain activity during regulation tasks can be linked to differences in self-control abilities. For example, trait measures of self-control correlated with both the ability to regulate negative emotions and enhanced functional connectivity between the amygdala and dorsolateral prefrontal cortex (dlPFC) (Paschke et al., 2016). Other studies have linked the desire for immediate reward to attenuated functional connectivity between cognitive control and reward-related brain regions such as the anterior prefrontal cortex and nucleus accumbens (Diekhof and Gruber, 2010; Diekhof et al., 2011; van den Bos et al., 2014; Moreno-Lopez et al., 2016). These findings are in line with work associating self-control abilities with connectivity of resting-state brain networks. For example, self-control

126 when making trade-offs between smaller, sooner monetary rewards and larger, later
127 ones was linked to enhanced resting-state connectivity between neural pathways
128 underpinning reward-processing and cognitive-regulation processes (Li et al., 2013).

129 Although associations between functional activation and self-control are tantalizing, it
130 is unclear whether individual differences in success are driven by momentary
131 fluctuations in motivation or attention, or by more stable, potentially neuroanatomical,
132 differences in the mechanisms of choice. Initial support for a neuroanatomical basis
133 comes from studies linking individual differences in structural connectivity between
134 reward-related and cognitive control areas to behavioral differences in impatience for
135 receiving monetary rewards (Peper et al., 2013; van den Bos et al., 2014). The goal of
136 the current paper was to further test this idea by investigating (1) whether differences
137 in neuroanatomy predict an individual's ability to regulate healthier dietary choices,
138 and if so (2) whether such differences depend on the type of regulatory strategy or are
139 generalizable across different strategies promoting healthier choices and participant
140 populations.

141 To answer these questions, we used voxel-based morphometry (VBM) to determine
142 whether and where neuroanatomical differences predict regulatory success during
143 dietary decisions that involve explicitly focusing on health goals. First, we aggregated
144 data from three independent studies (i.e., dataset 1), all employing a similar task that
145 prompted participants to regulate their dietary decision processes by focusing on the
146 healthiness of foods. Because subjective experience and behavior can be modified by
147 using distinct strategies with distinct consequences (Gross, 1998), we then tested
148 whether the same neuroanatomical variation underlies regulatory success for a
149 different regulation strategy. We addressed this second question by examining

structural predictors of regulatory success in a fully independent fourth study (i.e., dataset 2): participants in this study were not told to focus specifically on health attributes, but were instead encouraged to use a self-selected strategy to distance themselves from and reduce cravings for tasty but unhealthy foods (Hutcherson et al., 2012).

Our results indicate that neuroanatomical differences in specific value-related and cognitive control areas in the vmPFC and the dlPFC are generally predictive of regulatory success across different strategies and independent populations. They thus hold promise to serve as neuroanatomical markers of the ability to exercise self-control over dietary decisions.

Materials and Methods

Participants. The analyses included 123 healthy individuals (mean age: 29.97±0.96 years; 78 females, 45 males) from two different previously published studies (Hare et al., 2011; Hutcherson et al., 2012) and two different unpublished studies. Research was conducted in accordance with the Helsinki declaration and was approved by the local ethics committee (see Table 1 for an overview). All participants provided written and informed consent. Participants were screened for standard fMRI inclusion criteria: right-handedness, normal to corrected-to-normal vision, no history of substance abuse or any neurological or psychiatric disorder, and no medication or metallic devices. All participants were tested after four hours of fasting.

Procedure

Participants took part in one of two different dietary decision-making tasks that required them to use various strategies to make healthier choices.

173

174 *Regulation Task 1: Focusing on Healthiness of Foods (Dataset 1).*

175 Dataset 1 included 91 participants pooled over three similar studies (study 1: N = 13
176 from Hare et al., 2011; study 2: N = 35 from an unpublished study; study 3: N = 43
177 from another unpublished study) (see Table 1). Participants decided while in the fMRI
178 scanner how much they would like to eat different food items varying in tastiness and
179 healthiness at the end of the experiment. Participants made their choices under three
180 different conditions: being prompted to focus on (1) tastiness (TC) or (2) healthiness
181 (HC) of the foods or (3) with no dieting instruction (NC), i.e., making food choices as
182 they naturally would, which served as a baseline (see Figure 1a). Participants always
183 started with a baseline block (NC) followed by a randomized taste or health block.
184 The conditions were randomized across blocks of 10 trials, and participants were
185 instructed to rate how much they wanted to eat a food item presented on the screen
186 relative to a constant default option chosen for each participant. To determine the
187 weight participants placed on a food's tastiness and healthiness under different
188 regulatory goals, participants also indicated the perceived healthiness and tastiness of
189 all presented foods using a 4-point Likert scale (outside the scanner).

190 The tasks in studies 1, 2, and 3 were identical, with two exceptions. First, studies 1
191 and 3 consisted of 18 blocks of 10 trials (i.e., six blocks per condition of HC, TC,
192 NC), for a total of 180 trials. Study 2 consisted of 27 blocks of 10 trials (i.e., nine
193 blocks per condition of HC, TC, NC), for a total of 270 trials. Moreover, in study 2
194 the same food pictures were presented once in each condition of HC, TC, and NC.
195 Second, studies 1 and 2 included both men and women. Study 3 included only female

196 participants, who served as lean controls in a large-scale project aiming at the neural
197 and behavioral underpinnings of dietary decision-making in female obesity.

198 *Regulation Task 2: Distancing Oneself from Cravings for Unhealthy Foods (Dataset*
199 *2).* In a fourth study, 32 participants completed a different dietary self-control task
200 (Hutcherson et al., 2012). In study 4, rather than explicitly considering the healthiness
201 of food items, participants were instructed to distance themselves (distance condition,
202 or DC) from food cravings when contemplating highly palatable foods rich in calories
203 (see Figure 1c). (In separate blocks, participants in this study also attempted to
204 indulge their cravings for palatable, unhealthy foods; given the focus of this paper on
205 healthy food choices, these trials were not included in the current analyses.)
206 Participants were told to regulate their cravings by applying any strategy they
207 preferred. The task also had a baseline condition in which participants were asked to
208 make their dietary decisions naturally, without any regulation instruction (natural
209 condition, or NC). Fifty trials of each of the three conditions were randomly
210 intermixed, for a total of 150 trials. To make their decisions, participants were asked
211 to use a 6-point scale ($0, $0.50, $1, $1.50, $2, $2.50) to indicate their willingness to
212 pay (WTP) for the right to eat the food at the end of the experiment, rather than being
213 asked about how much they would like to eat it. Importantly, participants rated all
214 foods for subjective liking before entering the scanner, on the same scale used for
215 dataset 1. The high correlation between pre-scan liking and in-scan bids for foods in
216 the natural condition (average $r = .72 \pm .19$, $p < .001$) suggested that they measured
217 similar constructs.

218 To incentivize participants to choose according to their actual preferences, in *all four*
219 studies participants had to eat one item at the end of the experiment, determined by a

220 random draw of one trial. Food pictures were presented on a computer screen in the
221 form of high-resolution pictures (72 dpi). Matlab and Psychophysics Toolbox
222 extensions were used for stimulus presentation and response recording. Participants
223 saw the stimuli via goggles or a head-coil–based mirror and indicated their responses
224 using a response box system.

225 *Behavioral analyses.* All statistical tests were conducted with the Matlab Statistical
226 Toolbox (Matlab 2014a, MathWorks). In dataset 1, we measured regulatory success
227 by combining the increase in weight given to healthiness and the decrease in weight
228 given to tastiness during the health focus condition (HC), following the approach of
229 Hare et al., 2011. To this end, we fit a general linear model (GLM) to stimulus value
230 (SV, i.e., participants' ratings of how much they would like to eat a food item). The
231 behavioral GLM is described by equation *i*.

232 (i) $SV = \beta_0 + \beta_{HC}HC + \beta_{TC}TC + \beta_{HR}HR + \beta_{TR}TR + \beta_{HC\times HR}HC \times HR + \beta_{HC\times TR}HC \times$
233 $TR + \beta_{TC\times HR}TC \times HR + \beta_{TC\times TR}TC \times TR + \epsilon$

234 Stimulus value (SV) corresponded to the dependent variable, which was predicted by
235 the following regressors: HC, an indicator variable for a health focus condition block
236 (dummy coded); TC, an indicator variable for the taste focus condition block (dummy
237 coded); and HR and TR, corresponding to health rating and taste ratings for the trial-
238 specific food item (assessed outside the scanner). This GLM also included four
239 interaction terms: health focus condition by health rating (HCxHR), health focus
240 condition by taste rating (HCxTR), taste focus condition by health rating (TCxHR)
241 and taste focus condition by taste rating (TCxTR). Note that the TR and HR
242 regressors measure to what extent taste and health attributes of the food stimuli
243 influenced participants' stimulus values during the natural baseline condition (NC).

SV, TR, and HR regressors were scaled as –2 (strong no), –1 (no), 1 (yes), or 2 (strong yes). In contrast, the interaction terms (HCxHR, HCxTR, TCxHR, and TCxTR) assessed how much change occurred in the weight given to the taste and health attributes during the health or taste focus conditions, respectively. The individual regression coefficients (i.e., beta estimates β) for each regressor were analyzed at the group level using one-sample, two-tailed *t*-tests.

For the purpose of our subsequent analyses, equation *i* contains two terms of interest that characterize how participants regulated their food decisions to make healthier choices in the health condition (HC): (1) HCxHR, which assessed how much more participants integrated the healthiness of the food, and (2) HCxTR, which assessed how much the tastiness of the food was inhibited during the food decision. Because these two measures were highly correlated ($r = .53$, $p < .001$), we integrated them into an overall regulatory success score that was then entered as a regressor in the VBM analysis (i.e., $Regulatory\ Success_{\ dataset1} = \beta_{\mathrm{HCxHR}} - \beta_{\mathrm{HCxTR}}$). The more positive this difference score is, the higher the regulatory success of the participant.

The difference in SV (measured in this task as participants' WTP) between the natural condition and the distance condition was used as the measure of regulatory success ($i.e., Regulatory\ Success_{\ dataset2} = SV_{NC} - SV_{DC}$) for the 32 participants who took part in the second dietary decision-making task (i.e., dataset 2). This approach is the same as that originally used by Hutcherson et al. (2012). A positive score indicated that participants successfully regulated their cravings and exercised self-control because their SV for unhealthy foods was lower when they distanced themselves from their food cravings compared to their natural responses. A paired, two-tailed *t*-test was

conducted to test for a significant difference in SV between the distance and natural conditions.

MRI structural acquisition. Anatomical brain images were collected on a 3T Trio Siemens (studies 1, 2, 4) or a 3T Verio Siemens scanner (study 3). Whole-brain high-resolution T1 weighted structural scans (1 x 1 x 1 mm) were acquired for all 123 participants with a MPRAGE sequence. Details of the sequences are described in Table 1.

MRI data preprocessing. Each participant's anatomical image was segmented into gray matter (GM) using the SPM12 segmentation tool. Individual GM images were then co-registered between participants using Diffeomorphic Anatomical Registration through Exponentiated Lie Algebra (DARTEL). Next, the registered images were normalized to the Montreal Neurological Institute (MNI) stereotactic space using the DARTEL template, and spatially smoothed using a Gaussian kernel with full width at half maximum of 8 mm.

VBM analyses. All VBM analyses were performed using SPM12 (Wellcome Trust Center for Neuroimaging, http://www.fil.ion.ucl.ac.uk/spm). Out-of-sample predictions were conducted using the glmfit and glmval functions from the Matlab Statistical Toolbox (Matlab 2014a, MathWorks). We conducted GLM-based leave-one-subject-out (LOSO) predictive analyses within dataset 1 as well as cross-study predictions between datasets 1 and 2 to test whether individual differences in neuroanatomy were linked to dietary self-control choices. Building on the fMRI literature, our a priori focus was on GM volume in the dlPFC and vmPFC, but we

also tested models including additional regions for completeness. The details of the various analysis steps are given in the following paragraphs.

GM volume-based predictions of regulatory success within dataset 1. We conducted an out-of-sample LOSO prediction analysis for all participants in dataset 1 using the GLM described in equation ii.

$$\text{(ii) GM volume} = \beta_0 + \beta_{\text{reg\_success}} + \beta_{\text{age}} + \beta_{\text{gender}} + \beta_{\text{scanner}} + \beta_{\text{study1}} + \beta_{\text{study2}} + \beta_{\text{study3}} + \beta_{\text{global GM}} + \epsilon$$

The beta estimate, $\beta_{\text{reg\_success}}$, quantifying the relationship between the change in regulatory success during the health focus condition (i.e., $(\beta_{\text{HCxHR}} - \beta_{\text{HCxTR}})$ from the behavioral regression (Eq. i)) and voxel-wise GM volume was our effect of interest. Note that regulatory success is expected to increase with a positive value for β_{HCxHR} or a negative value for β_{HCxTR} so the subtraction $(\beta_{\text{HCxHR}} - \beta_{\text{HCxTR}})$ quantifies the total increase in regulatory success. Voxels in which GM volume was potentially predictive of regulatory success were identified by the contrast $[\beta_{\text{reg\_success}} > 0]$. To control for variance related to age, gender, MRI scanner, study, and global GM volume, these factors were included in all voxel-wise linear regression models (following ANCOVA normalization).

The LOSO procedure was conducted as follows: We divided dataset 1 into 91 separate training (90 participants) and test (1 participant) sets. For each training set, we computed the GLM described by Eq. *ii* above. We then created 91 sets of ROIs from these results using a voxel-wise threshold of $t = 2.64$ ($p < 0.005$). Each set of contiguous voxels was treated as a single ROI, and GM volume was averaged over the voxels in each ROI. Next, we used these 91 sets of independently defined ROI

masks to calculate a predicted regulatory success measure for each participant in dataset 1 using the GLMs in equations *iii* and iii_{all}. These GLMs differed in terms of whether they used only our a priori regions of interest, dlPFC and vmPFC, or all ROIs identified in a particular training set to predict regulatory success in the left-out participant.

(iii) $$regulatory\ success = \beta_0 + \beta_{dlPFC} * GM_{dlPFC} + \beta_{vmPFC} * GM_{vmPFC} + \epsilon$$

(iii_{all}) $$regulatory\ success = \beta_0 + \beta_{dlPFC} * GM_{dlPFC} + \beta_{vmPFC} * GM_{vmPFC} + \beta_X * GM_X + \epsilon$$

In both GLMs, the subscripts dlFPC and vmPFC refer to the GM volume from those two regions. We assigned anatomical labels based on the MNI coordinates to each set of 91 ROIs allowing us to identify the dlPFC and vmPFC in each set. Both dlPFC and vmPFC ROIs were present in all 91 training sets. For equation iii_{all}, the subscript X refers to potential additional regressors for any additional ROIs present in that specific training set.

Last, once we had obtained a predicted regulatory success value for each participant from equation *iii* or iii_{all}, we quantified the association between predicted and observed regulatory success using Pearson's correlation and a permutation test, which involved estimating the distribution of correlation coefficients by randomly resampling with replacement 10,000 observations for observed and predicted regulatory success.

Predicting out-of-sample regulatory success at the participant and task levels. We also tested whether regulatory success can be predicted in an independent sample of participants (dataset 2, N = 32) performing a different regulation task (i.e., regulation

task 2). First, we computed the average GM volume values for each participant in dataset 1 within 5-mm-radius spheres centered around the peak MNI coordinates found within the dlPFC (MNI [40, 40, 20]) and vmPFC (MNI [9, 46, –15]) when estimating Eq. *ii* for the full participant sample in dataset 1. Second, we computed the GLM in Eq. *iii* across all dataset 1 participants in order to estimate the relationship (i.e. beta coefficients β_{dlPFC} and β_{vmPFC}) between vmPFC and dlPFC GM volume and regulatory success. Next, we tested whether regression weights estimated for dataset 1 ($\beta_{dlPFC} = 6.68, \beta_{vmPFC} = 6.92, \beta_0 = 0.0002$) could significantly predict regulatory success on the separate behavioral task used in dataset 2 when combined with the dlPFC and vmPFC GM volumes of those participants. In other words, we used Eq. *iii* with the intercept set to 0.0002 and GM volume beta coefficients for dlPFC set to 6.68 and for vmPFC set to 6.92 to make predictions about regulatory success in dataset 2. Last, we used Pearson's correlation and the same permutation test that was used for testing the results of Eqs. *iii* and iii_{all} in dataset 1 to quantify the association between the predicted and observed levels of regulatory success (SV(NC − DC)) in dataset 2.

Voxel-wise correlations with regulatory success in dataset 2. To test the relationship between GM volume and regulatory success within dataset 2, we conducted a voxel-wise GLM analysis on these data using equation *iv* below.

(iv) $$GM\ volume\ = \beta_0 + \beta_{reg\_success} + \beta_{age} + \beta_{gender} + \beta_{global\ GM} + \epsilon$$

This model mirrored the model in Eq. *ii* except that it omitted study and scanner dummy regressors because all participants in the dataset were part of the same study and thus were scanned with the same MRI scanner. Regulatory success in Eq. *iv* was defined as difference in average SV during the natural condition (NC) compared to

the distance condition (DC) (i.e., $Regulatory\ Success_{\ dataset2} = SV_{NC} - SV_{DC}$). Once again, voxels in which GM volume was positively associated with regulatory success were identified by the contrast [$\beta_{reg\_success} > 0$].

Results

Behavioral results

Regulatory success when focusing on healthiness during SV computations in dataset 1. We quantified regulatory success in terms of how much participants adjusted the relative weights on healthiness and tastiness in the health focus compared to the natural condition (i.e., the HCxHR and HCxTR interaction terms shown in Figure 1b). In line with the previously reported results in the separate original studies, the behavioral GLM described in Eq. *i* showed significant interactions between the weightings of the health and taste attributes and the choice conditions in the joint set of 91 participants (Table 2).

These interaction terms capture different forms of regulatory success. Health attributes were significantly more integrated into SV computations in the health focus condition ($ß_{HCxHR} = 0.39$, $SEM_{HCxHR} = 0.04$, $t(90) = 10.8$, $p < .001$), indicating that *more* weight was placed on the healthiness of the foods compared to natural condition. Taste attributes of the foods were significantly less integrated into SV computations in the health focus condition ($ß_{HCxTR} = –0.25$, $SEM_{HCxTR} = 0.03$, $t(90) = –7.74$, $p < .001$), indicating that *less* weight was placed on the tastiness of the foods compared to the natural condition. The changes in the influence of taste ($ß_{HCxTR}$) and healthiness ($ß_{HCxHR}$) on SV between HC and NC conditions were significantly

correlated across subjects ($r = .53$, $p < .001$). Although our primary interest is in the differences between HC and NC conditions, we note that there was a significant TCxHR interaction ($\beta_{TCxHR} = –0.06$, $SEM_{TCxHR} = 0.02$, $t(90) = –2.91$, $p = .005$) as well, such that participants were less sensitive to the healthiness of foods in the TC condition. There was no significant TCxTR interaction.

Regulatory success during SV computation using distancing strategies in dataset 2. Here we briefly restate the behavioral results for participants from dataset 2. These results are the same as those originally reported in Hutcherson et al. (2012), but are repeated here for the reader's convenience. Participants in dataset 2 showed significantly higher SV in the indulge ($M_{IC\_zscored} = 0.25$, $SEM_{IC\_zscored} = 0.04$) versus the natural condition ($t(31) = 6.22$, $p < .001$, 95% CI: 0.17, 0.33). In contrast, they showed significantly lower SV in the distancing condition (mean $SV_{DC\_zscored} = –0.25$, $SEM_{DC\_zscored} = 0.04$) compared to the natural condition (mean $SV_{NC\_zscored} = –0.002$, $SEM_{NC\_zscored} = 0.02$; $t(31) = –6.69$, 95% CI: –0.32 ,–0.17, $p < .001$; see Figure 1d). We used this difference in SV between the distancing and the natural control conditions as the measure of regulatory success for our further analyses in this paper.

VBM results

Anatomical predictors of regulatory success when focusing on healthiness. We were able to significantly predict regulatory success in dataset 1 using GM volume in independently defined dlPFC and vmPFC ROIs and regression weights in a leave-one-subject-out procedure. When basing the prediction of regulatory success on information from dlPFC and vmPFC alone, there was a significant *positive* association between predicted and observed regulatory success (Pearson's $r = 0.25$, $p = 0.02$, 95% CI due to chance: –0.17, 0.17, see Figure 2a). In contrast, when using all

regions that were correlated with regulatory success in a given training set to predict regulatory success in the test set, there was no significant correlation (Pearson's r = –0.16, p = .11, 95% CI due to chance: –0.17, 0.17, see Figure 2a). The generalization failure of models trained using the GM volume from additional brain regions indicates that these models may be overfitting to the training set. Our results are in line with fMRI studies that have frequently reported the recruitment of the vmPFC and the dlPFC in dietary choices made under both regulatory goals and unregulated conditions (Plassmann et al. 2007, 2010, Hare et al., 2009, 2011; Hutcherson et al., 2012; Harris et al., 2013; van der Laan et al, 2014). In light of these results, we focused on these two regions when attempting to predict regulatory success across choice paradigms using neuroanatomy.

Anatomical markers of regulatory success across regulation strategies and populations. Next we tested whether the neuroanatomical correlates of regulatory success identified in regulation task 1 and dataset 1 could be used to make predictions about regulatory success in a separate set of individuals attempting to engage self-regulation in a different type of food choice paradigm (i.e., regulation task 2). In other words, we sought to test how predictive and generalizable the associations between dlPFC and vmPFC GM volume and self-regulation were (see Figure 2b). Thus, we computed beta weights quantifying the association between dlPFC (β_{dlPFC} = 6.68) and vmPFC (β_{vmPFC} = 6.92) GM volumes ($\beta_0 = 0.0002$) and the regulatory success measure obtained in dataset 1 (i.e., Eq. *iii*), and then used these weights together with the GM volumes measured in these regions for participants in dataset 2 to predict regulatory success in dataset 2. We found that there was a significant correlation between GM-predicted and observed regulatory success (Figure 2b; Pearson's r = 0.35, p = 0.04, 95% CI of correlations due to chance: –0.29, 0.29), indicating that the

combination of dlPFC and vmPFC GM volumes can be used to generate significant out-of-sample predictions of regulatory success in different tasks. For robustness, we checked whether the dlPFC and vmPFC separately predicted out-of-sample regulatory success by correlating predicted regulatory success calculated based on the beta weight and GM volume of each of the two ROIs, respectively. The Pearson correlations between predicted and observed regulatory success were $r = 0.28$, $p = 0.11$ for the dlPFC and $r = 0.34$, $p = 0.06$ for the vmPFC. Fisher's r-to-z transformation did not detect any significant differences between the two correlations ($z = -0.34$, $p = 0.73$, two-tailed).

Whole-brain, voxel-wise regression analyses. We also ran exploratory whole-brain, voxel-wise VBM analyses across all participants within both datasets 1 and 2 separately. No regions survived correction for multiple comparisons in either dataset (see Tables 3 and 4). For illustrative purposes, in Figure 2c we plot voxels in which GM volume correlated with regulatory success in the respective tasks for datasets 1 and 2.

Discussion

Making healthy food choices is often a challenge in everyday life, and people vary in their ability to choose healthy over tasty foods on the menu, even when they have the explicit goal of eating healthily. This paper provides new evidence that regulatory success in healthy eating is related, in part, to individual differences in brain anatomy in both the vmPFC and dlPFC. Importantly, this relationship generalizes across different groups and regulatory strategies. These findings suggest that both brain regions contribute broadly to the regulation of valuation processes in the context of dietary decision-making and its control.

Implications for dietary decision-making and self-control

Our findings are relevant for current neuroeconomic theories of dietary self-control. Some research in this area suggests that the vmPFC and the dlPFC may represent distinct value systems biased to respond to either immediate hedonistic rewards or delayed, more abstract rewards (McClure et al., 2004; Hutcherson et al., 2012). Other research suggests a more cooperative relationship, in which the dlPFC modulates computations in the vmPFC in order to weight different attributes according to current behavioral goals (Hare et al., 2009). Consistent with both theoretical accounts, our results suggest a key role of the vmPFC and the dlPFC for dietary self-control on an *anatomical* level.

Limitations and open questions

Our work has several limitations. First, our results do not speak to the question of whether the vmPFC and the dlPFC play differentiable or similar roles in regulatory success. Understanding their specific roles and their interactions is important because of an ongoing debate in the literature regarding different models of self-control: Do they represent two independent sources of value (McClure et al., 2004; Hutcherson et al., 2012), or does the dlPFC play only an indirect role in choice by modulating value signals within the vmPFC (Hare et al., 2009, 2011)? Our results are fully consistent with both models, because dlPFC gray matter volume could either contribute an independent value input to choice processes or provide enhanced capacity to modulate vmPFC value signals. Further work will be needed to tease apart the common and distinct roles the dlPFC and the vmPFC play in regulatory success.

For example, approaches using patients with localized lesions in these brain areas or methods that temporarily inhibit or excite brain activity in these regions will be

477 particularly important. Evidence for a causal role of both regions in human decision-
478 making already exists. For example, transcranial magnetic stimulation (TMS) of the
479 dlPFC produces clear alterations in choice behavior, both in the context of foods
480 (Camus et al., 2009) and in the context of intertemporal decision-making (Figner et
481 al., 2010). Although this latter result is not directly related to healthy decision-
482 making, intertemporal considerations may still play an important role in food choice,
483 which involves trade-offs between the immediately rewarding taste and longer-term
484 benefits of healthiness in dietary choices. Causal evidence for the role of the vmPFC
485 in dietary and monetary intertemporal choices comes from lesion studies (Sellitto et
486 al., 2010; Camille et al., 2011; Jo et al., 2013; Peters and D'Esposito, 2016). Taken
487 together then, our results and the results of lesion studies confirm a critical role for
488 both the vmPFC and the dlPFC, but future research investigating their potentially
489 dissociable roles is needed.

490 Another important question raised by our results is how generalizable the role of
491 individual differences in dlPFC and vmPFC neuroanatomy is beyond the realm of
492 dietary choices. For example, do dlPFC and vmPFC gray matter volumes also predict
493 self-control success for financial decisions when considering saving for the future
494 instead of consuming now? There is evidence indicating that individual differences in
495 dlPFC neuroanatomy are related to regulating the intake of addictive substances
496 (Holmes et al., 2016), suggesting a broad and generalizable role for the dlPFC.

497 ***Conclusion***

498 Our findings extend previous work by highlighting the importance of individual
499 differences in the *neuroanatomy* of the dlPFC and the vmPFC for dietary decision-
500 making and its control. They imply that individual differences in the dlPFC and

vmPFC anatomy could be combined with existing assays and measures such as choice, fMRI, or questionnaire data to better estimate an individual's likelihood of success in regulating dietary choices. Our results suggest that regulatory success may result not only from momentary fluctuations in motivation and attention, but also from more stable variation in neuroanatomy.

Yet the brain and its anatomy are also subject to plasticity in response to new situations, life styles, disease, and environmental constraints (Merzenich et al., 2013). An exciting avenue going forward will be to explore whether self-control training or biofeedback methods could harness neural plasticity to yield long-lasting changes in self-regulatory capacity. Our results suggest that the dlPFC and vmPFC may represent key targets for interventions that alter disadvantageous dietary choices in at-risk populations (e.g., those with obesity or eating disorders).

513 **References**

514 Camille N, Griffiths CA, Vo K, Fellows LK, Kable JW (2011) Ventromedial frontal lobe damage
515 disrupts value maximization in humans. J Neurosci 31(20):7527–7532.

516 Camus M, Halelamien N, Plassmann H, Shimojo S, O'Doherty J, Camerer C, Rangel A (2009)
517 Repetitive transcranial magnetic stimulation over the right dorsolateral prefrontal cortex decreases
518 valuations during food choices. Eur J Neurosci 30:1980–1988.

519 Diekhof EK, Gruber O (2010) When desire collides with reason: Functional interactions between
520 anteroventral prefrontal cortex and nucleus accumbens underlie the human ability to resist
521 impulsive desires. J Neurosci 30:1488–1493.

522 Diekhof EK, Nerenberg L, Falkai P, Dechent P, Baudewig J, Gruber O (2011) Impulsive personality
523 and the ability to resist immediate reward: An fMRI study examining interindividual differences
524 in the neural mechanisms underlying self-control. Hum Brain Mapp 33:2768–2784.

525 Figner B, Knoch D, Johnson EJ, Krosch AR, Lisanby SH, Fehr E, Weber EU (2010) Lateral prefrontal
526 cortex and self-control in intertemporal choice. Nat Neurosci 13:538–539.

527 Hare TA, Camerer CF, Rangel A (2009) Self-control in decision-making involves modulation of the
528 vmPFC valuation system. Science 324:643–646.

529 Hare TA, Malmaud J, Rangel A (2011) Focusing attention on the health aspects of foods changes value
530 signals in vmPFC and improves dietary choice. J Neurosci 31:11077–11087.

531 Harris A, Hare T, Rangel A (2013) Temporally dissociable mechanisms of self-control: Early
532 attentional filtering versus late value modulation. J Neurosci 33:18917–18931.

533 Holmes AJ, Hollinshead MO, Roffman JL, Smoller JW, Buckner RL (2016) Individual differences in
534 cognitive control circuit anatomy link sensation seeking, impulsivity, and substance use. J
535 Neurosci 36:4038–4049.

536 Hutcherson CA, Plassmann H, Gross JJ, Rangel A (2012) Cognitive regulation during decision making
537 shifts behavioral control between ventromedial and dorsolateral prefrontal value systems. J

538 Neurosci 32:13543–13554.

539 Gross JJ (1998) The emerging field of emotion regulation: An integrative review. Rev Gen Psychol
540 2(3):271–299.

541 Jo S, Kim K-U, Lee D, Jung MW (2013) Effect of orbitofrontal cortex lesions on temporal discounting
542 in rats. Behav Brain Res 245:22–28.

543 Jung-Beerman M, Bowden EM, Haberman J, Frymiare JL, Arambel-Liu S, Greenblatt R, Reber PJ,
544 Kounios J (2004). Neural activity when people solve verbal problems with insight. PLoS Biol
545 2(4):E97.

546 Kable JW, Glimcher PW (2007) The neural correlates of subjective value during intertemporal choice.
547 Nat Neurosci 10:1625–1633.

548 Kober H, Kross EF, Mischel W, Hart CL, Ochsner KN (2010) Regulation of craving by cognitive
549 strategies in cigarette smokers. Drug Alcohol Depend 106:52–55.

550 Kuchinke L, Fritzemeier S, Hofmann MJ, Jacobs AM (2013) Neural correlates of episodic memory:
551 Associative memory and confidence drive hippocampus activations. Behav Brain Res 254:92–
552 101.

553 Li N, Ma N, Liu Y, He XS, Sun DL, Fu XM, Zhang X, Han S, Zhang DR (2013) Resting-state
554 functional connectivity predicts impulsivity in economic decision-making. J Neurosci 33:4886–
555 4895.

556 McClure SM, Laibson DI, Loewenstein, G, Cohen JD (2004) Separate neural systems value immediate
557 and delayed monetary rewards. Science 306:503–507.

558 Merzenich M, Nahum M, Van Vleet TM (2013) Changing brains: Applying brain plasticity to advance
559 and recover human ability. Progress in Brain Research, vol. 207. Amsterdam: Elsevier.

560 Moreno-Lopez L, Contreras-Rodriguez O, Soriano-Mas C, Stamatakis EA, Verdejo-Garcia A (2016)
561 Disrupted functional connectivity in adolescent obesity. Neuroimage Clin 12:262–268.

562 Paschke LM, Dörfel D, Steimke R, Trempler I, Magrabi A, Ludwig VU, Schubert T, Stelzel C, Walter

563 H (2016) Individual differences in self-reported self-control predict successful emotion regulation.
564 Soc Cogn Affect Neurosci 11:1193–1204.

565 Peper JS, Mandl RCW, Braams BR, de Water E, Heijboer AC, Koolschijn PCMP, Crone EA (2013)
566 Delay discounting and frontostriatal fiber tracts: A combined DTI and MTR study on impulsive
567 choices in healthy young adults. Cereb Cortex 23:1695–1702.

568 Peters J, D'Esposito M (2016) Effects of medial orbitofrontal cortex lesions on self-control in
569 intertemporal choice. Curr Biol 26:2625–2628.

570 Pietilaeinen KH, Saarni SE, Kaprio J, Rissanen A (2011) Does dieting make you fat? A twin study. Int
571 J Obes Relat Metab Disord 36:456–464.

572 Plassmann H, O'Doherty, J., Rangel A (2007) Orbitofrontal cortex encodes willingness to pay in
573 everyday economic transactions. J Neurosci 27:9984-9988.

574 Plassmann H, O'Doherty, J., Rangel A (2010) Appetitive and aversive goal values are encoded in the
575 medial orbitofrontal cortex at the time of decision making. J Neurosci 32: 10799-10808.

576 Saarni SE, Rissanen A, Sarna S, Koskenvuo M, Kaprio J (2006) Weight cycling of athletes and
577 subsequent weight gain in middle age. Int J Obes Relat Metab Disord 30:1639–1644.

578 Sellitto M, Ciaramelli E, di Pellegrino G (2010) Myopic discounting of future rewards after medial
579 orbitofrontal damage in humans. J Neuro 30:16429–16436.

580 Tangney JP, Baumeister RF, Boone AL (2004) High self-control predicts good adjustment, less
581 pathology, better grades, and interpersonal success. J Pers 72:271–322.

582 van den Bos W, Rodriguez CA, Schweitzer JB, McClure SM (2014) Connectivity strength of
583 dissociable striatal tracts predict individual differences in temporal discounting. J Neurosci
584 34:10298–10310.

585 van der Laan LN, de Ridder DTD, Viergever MA, Smeets PAM (2014) Activation in inhibitory brain
586 regions during food choice correlates with temptation strength and self-regulatory success in
587 weight-concerned women. Front Neurosci 8:308.

Figure legends

Figure 1. Experimental design and behavioral results. ***A*:** Behavioral task dataset 1. Screenshots display successive events within one trial of each condition (i.e., health focus [HC], taste focus [TC], and natural focus [NC] conditions) during the dietary decision-making task performed by the participants of dataset 1 with durations in seconds. Conditions were presented in blocks, randomly intermixed. Each block started with an instruction to focus attention on the healthiness, taste, or natural preference. Next, a food item was displayed on the screen and participants had to evaluate how much they would like to eat it by pressing buttons corresponding to *strong no*, *no*, *yes*, and *strong yes*. ***B*:** Behavioral results in dataset 1 (N = 91). The bar graph depicts mean beta estimates for each regressor of equation i. The dotted red lines indicate the behavioral measures of interest: the weight of the healthiness [HR] and the tastiness [TR] on stimulus value computation during the health focus condition [HC]. ***C*:** Behavioral task dataset 2. Screenshots display successive events within one trial of each condition (i.e., distance [DC], indulge [IC], and natural [NC] conditions) during the dietary decision-making task performed by the participants of dataset 2 with durations in seconds. Conditions were presented in blocks, randomly intermixed. Each block started with an instruction to try to distance oneself from food cravings, indulge in food cravings, or make decisions naturally. Next, a food item was displayed on the screen and participants had to evaluate how much they would be willing to pay for the food item by pressing buttons corresponding to *$0*, *$0.50*, *$1*, *$1.50*, *$2*, and *$2.50*. ***D,*** Behavioral results in dataset 2 (N = 32). The bar graph depicts mean stimulus value of food items in each condition. The asterisks (*) indicate significance against zero at $p < 0.05$. HCxHR: interaction of healthiness ratings with the health focus condition; HCxTR: interaction of taste ratings with the health focus condition; TCxHR: interaction of the healthiness ratings with the taste focus condition; TCxTR: interaction of taste ratings with the taste focus condition. **HR:** healthiness ratings; TR: tastiness ratings. Error bars are ± intersubject standard errors of the mean (SEM).

Figure 2. Neuroanatomical markers of regulatory success in dataset 1 and dataset 2. *A*: Correlation between predicted and observed regulatory success for out-of-sample participants of dataset 1 when considering all clusters (left panel, Pearson's $r = -0.16$, $p = 0.11$) or only vmPFC and dlPFC clusters (right panel, Pearson's $r = 0.25$, $p = 0.02$). Dots correspond to participants. *B*: Correlation between predicted and observed regulatory success for out-of-sample participants of dataset 2 when considering only the weights of the vmPFC and dlPFC clusters identified in dataset 1. *C:* GM volume in the dlPFC and vmPFC significantly correlated with overall regulatory success score (i.e., $ß_{HCxHR} - ß_{HCxTR}$) of dataset 1 (N = 91, illustrated in red) and of dataset 2 (i.e., $SV_{(NC-DC)}$, N = 32, illustrated in yellow). Significant voxels are displayed for visualization purposes at a whole-brain threshold of $p < 0.005$ uncorrected. SPMs are superimposed on the average structural brain image of each sample, respectively.

Table 1: Study and dataset overview

Study	Data set	Local ethics committee	Scanner	MPRAGE sequence	N	Age (SEM)	Female :male	Task condition	DV	Other ratings
1	1	California Institute of Technology (Pasadena, CA)	3T Trio Siemens	TR = 1.5 s; TE = 3.05 ms; 176 sagittal slices; 256x256 matrix	13*	38.2 (12.8)	8:5	health, natural, taste	SV	health, taste
2	1	California Institute of Technology (Pasadena, CA)	3T Trio Siemens	TR = 1.5 s; TE = 2.91 ms; 176 sagittal slices; 256x256 matrix	35	29 (0.9)	16:19	health, natural, taste	SV	health, taste
3	1	Comité de Protection des Personnes, Ile-de-France VI, INSERM approval #C07-28, DGS approval #2007-0569, IDRCB approval #2007-A01125-48CPP	3T Verio Siemens	TR = 2.3 s; TE = 2.98 ms; 176 sagittal slices; 240x256 matrix	43	24.8 (5.1)	43	health, natural, taste	SV	health, taste
4	2	California Institute of Technology (Pasadena, CA)	3T Trio Siemens	TR = 1.5 s; TE = 3.05 ms; 176 sagittal slices; 256x256 matrix	32	22 (3.3)	11:21	distance, natural, indulge	W TP	food liking

DV: dependent variable; SV: stimulus value; WTP: willingness to pay. *Note that information on the gender and age for 20 out of the original 33 participants in the Hare et al. (2011) study was no longer available. Therefore, we included only the 13 participants from that study for whom we had all relevant information for the data analysis.

Table 2: Multiple regression results on stimulus value (SV) in dataset 1

Study 1	**Intercept**	**HR**	**TR**	**HC**	**TC**	**HCxHR**	**TCxHR**	**HCxTR**	**TCxTR**
Coeff	–0.01	0.14	0.61	–0.20	–0.01	0.24	–0.06	–0.20	0.05
STE	0.07	0.04	0.05	0.06	0.04	0.05	0.03	0.06	0.03
t	–0.12	3.88	13.25	–3.36	–0.17	4.93	–2.02	–3.67	1.59
Z	–1.32	3.27	7.50	–2.86	–1.11	4.02	–1.61	–3.12	1.16
p	0.9061	0.0005	0.0000	0.0021	0.8656	0.0000	0.0532	0.0009	0.1231
Study 2	**Intercept**	**HR**	**TR**	**HC**	**TC**	**HCxHR**	**TCxHR**	**HCxTR**	**TCxTR**
Coeff	0.24	–0.06	0.26	–0.28	0.08	0.28	–0.06	–0.19	0.01
STE	0.08	0.03	0.03	0.07	0.03	0.04	0.02	0.03	0.02
t	2.93	–2.28	9.36	–3.83	2.32	6.54	–2.89	–5.68	0.34
Z	2.51	–1.90	6.43	–3.27	1.94	5.09	–2.47	–4.58	0.64
p	0.0060	0.0287	0.0000	0.0005	0.0264	0.0000	0.0067	0.0000	0.7387
Study 3	**Intercept**	**HR**	**TR**	**HC**	**TC**	**HCxHR**	**TCxHR**	**HCxTR**	**TCxTR**
Coeff	–0.13	0.06	0.28	–0.16	0.11	0.26	–0.04	–0.20	–0.04
STE	0.07	0.03	0.04	0.06	0.04	0.04	0.03	0.05	0.04
t	–1.75	1.96	7.70	–2.50	2.52	6.67	–1.25	–4.38	–0.96
Z	–1.35	1.58	5.87	–2.13	2.15	5.22	–0.78	–3.75	–0.41
p	0.0878	0.0571	0.0000	0.0165	0.0159	0.0000	0.2190	0.0001	0.3406
all 3 studies	**Intercept**	**HR**	**TR**	**HC**	**TC**	**HCxHR**	**TCxHR**	**HCxTR**	**TCxTR**
Coeff	0.06	0.02	0.36	–0.24	0.08	0.39	–0.06	–0.25	0.00
STE	0.05	0.03	0.03	0.04	0.02	0.04	0.02	0.03	0.02
t	1.18	0.75	12.95	–5.57	3.30	10.88	–2.91	–7.74	0.16
Z	0.70	0.11	8.13	–5.01	2.99	8.13	–2.60	–6.62	1.14
p	0.2408	0.4543	0.0000	0.0000	0.0014	0.0000	0.0047	0.0000	0.8735

The table depicts results from Eq. *i* fitted to SV for each of the three studies of dataset 1 separately and for all three studies taken together. The two interactions HCxHR and HCxTR are highlighted by red lines, because they were the main regressors of interest and were used to calculate a combined regulatory success measure.

Table 3: VBM results in N = 91 participants (dataset 1): Positive effect of regulatory success

Region	BA	x	y	z	Peak z-score
dlPFC	46	40	40	20	3.74
dmPFC	6	15	18	57	3.70
		18	25	60	3.20
STG	22	60	2	0	3.22
mPFC	10	4	64	0	3.08
vmPFC	25/11	9	46	–15	2.99

This table reports the peak coordinates and z-score values for the VBM analysis detailed in Eq. *ii* across the full sample of 91 participants in dataset 1. All peaks surpassing a voxel-wise threshold of $p < 0.001$ uncorrected are reported for completeness, but only the dlPFC and vmPFC ROIs were used to predict regulatory success across samples. Note that this table is provided as an overview of the results of Eq. *ii* when fit to dataset 1 and the locations of the dlPFC and vmPFC ROIs used to predict regulatory success in dataset 2, but is not the basis of any statistical inferences in this manuscript. The xyz coordinates correspond to the Montreal Neurological Institute (MNI) space. dlPFC: dorsolateral prefrontal cortex; dmPFC: dorsomedial prefrontal cortex; STG: superior temporal gyrus; mPFC: medial prefrontal cortex; vmPFC: ventromedial prefrontal cortex.

Table 4: VBM results in N = 32 participants (dataset 2): Positive effect of regulatory success

Region	BA	x	y	z	Peak z-score
dlPFC	46/10	42	43	15	4.25
ACC	32/9	–12	40	18	4.06
		14	40	2	3.37
dACC		0	18	36	3.28
PCG	4	55	–9	45	4.03
	6	55	–3	12	3.42
vmPFC	25	10	34	–15	3.70
	11	2	26	–8	3.18
AG	39	44	–56	21	3.43

This table was obtained by a VBM analysis with a combined regulatory success as a predictor variable of GM volume (Eq. *iv*) using a whole-brain threshold of $p < 0.001$ uncorrected. The xyz coordinates correspond to the Montreal Neurological Institute (MNI) space. dlPFC: dorsolateral prefrontal cortex; ACC: anterior cingulate cortex; dACC: dorsal anterior cingulate cortex; PCG: precentral gyrus; AG: angular gyrus; vmPFC: ventromedial prefrontal cortex.

a

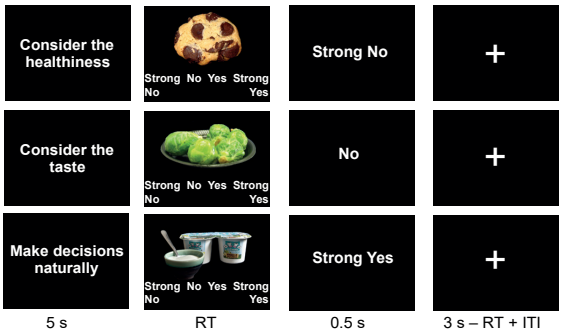

b

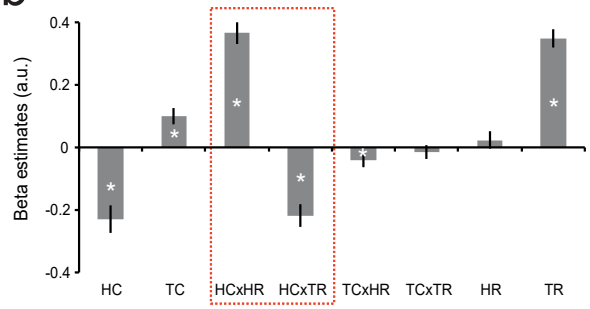

c

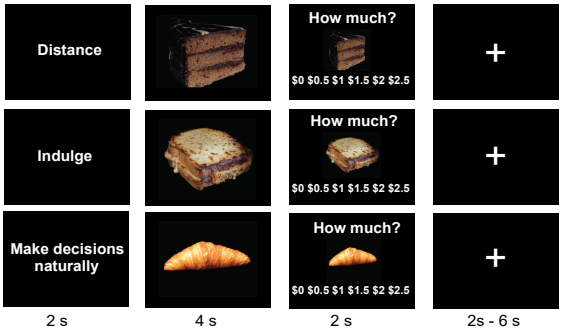

d